



# Assessment of air quality before and during the COVID-19 and its potential health impacts in an arid oasis city: Urumqi, China

Yaxin Sun<sup>1,2</sup> · Tayierjiang Aishan<sup>1,2</sup> · Ümüt Halik<sup>1,2</sup> · Florian Betz<sup>3</sup> · Remila Rezhake<sup>4</sup>

Accepted: 2 November 2022 / Published online: 18 November 2022

© The Author(s), under exclusive licence to Springer-Verlag GmbH Germany, part of Springer Nature 2022

## Abstract

As a key node city of the “Silk Road Economic Belt” Urumqi has been listed as one of the ten most polluted cities in the world, posing a serious threat to the urban environment and residents’ health. This study analyzed the air quality before and during the COVID-19 (Coronavirus disease 2019) pandemic and its potential health effects based on the data of PM<sub>2.5</sub>, PM<sub>10</sub>, SO<sub>2</sub>, NO<sub>2</sub>, CO, and O<sub>3\_8h</sub> levels from 10 air quality monitoring stations in Urumqi from January 1, 2017, to December 31, 2021. As per the results, the concentrations of the air pollutants PM<sub>2.5</sub>, PM<sub>10</sub>, SO<sub>2</sub>, NO<sub>2</sub>, CO, and O<sub>3\_8h</sub> in Urumqi from 2017 to 2021 showed a cyclical trend, and the implementation of COVID-19 prevention and control measures could effectively reduce the concentration( $\rho$ ) of air pollutants. The mean value of  $\rho$ (PM<sub>2.5</sub>) decreased from 2017 to 2021, whereas  $\rho$ (O<sub>3\_8h</sub>) showed a waveform change trend (increased in 2017–2018, decreased in 2018–2020, and increased after 2020). Meanwhile, the maximum annual average values of  $\rho$ (PM<sub>2.5</sub>) and  $\rho$ (O<sub>3\_8h</sub>) for the six monitoring stations during 2017–2021 occurred at sites S2 (74.37  $\mu\text{g m}^{-3}$ ) and S6 (91.80  $\mu\text{g m}^{-3}$ ), respectively; rapid industrialization had a greater impact on PM<sub>2.5</sub> and O<sub>3\_8h</sub> concentrations compared to commercial and residential areas. In addition, the air quality index data series can characterize the fluctuation trend of PM<sub>2.5</sub>. The high pollution levels (Class IV and V) of the air pollutants PM<sub>2.5</sub> and O<sub>3\_8h</sub> in Urumqi have been decreasing annually, and good days can account for 80–95% of the total number of days in the year, indicating that the number of days with a potential threat to residents’ health is gradually decreasing. Therefore, more attention should be paid in controlling and managing air pollution in Urumqi.

**Keywords** Air pollution · PM<sub>2.5</sub> · Human health · Oasis city · COVID-19 · Urumqi

## 1 Introduction

Air pollution is the main cause of environmental quality deterioration in many cities around the world (Sofia et al. 2020; Ambade et al. 2021a, b), which not only adversely affects human health but also poses a threat to sustainable

socio-economic development and even contributes to global warming (Almetwally et al. 2020; Du et al. 2019). According to the International Organization for Standardization (ISO), air pollution refers to the phenomenon in which the concentration of certain substances in the air reaches a threshold within a certain period, thereby causing damage to human health or the ecological environment (<https://www.iso.org/home.html>).

With rapid economic growth, the expansion of industrialization and urbanization, and the surge in population density, urban air pollution has become increasingly serious, exposing many residents to health risks (Chen and Chen 2021; Du et al. 2018; Jiang and Bai 2018; Xu et al. 2022). According to the latest statistics, air pollution has become the fourth leading risk factor for death in China after heart attack, dietary risk, and smoking (Jiang and Bai 2018). The level of air pollutants in Chinese cities is much higher than that recommended by the World Health

✉ Tayierjiang Aishan  
tayirjan@xju.edu.cn

<sup>1</sup> College of Ecology and Environment, Xinjiang University, Urumqi 830046, Xinjiang, China

<sup>2</sup> Ministry of Education Key Laboratory of Oasis Ecology, Urumqi 830046, Xinjiang, China

<sup>3</sup> Faculty of Mathematics and Geography, University of Eichstaett-Ingolstadt, Ostenstraße 14, 85071 Eichstaett, Germany

<sup>4</sup> Affiliated Cancer Hospital of Xinjiang Medical University, Urumqi 830017, Xinjiang, China

Organization (WHO) (He et al. 2017). Furthermore, seven of the top ten most polluted cities in the world are located in China (Chen and Chen 2021). Cities consume 20% of the global energy, and the production of this energy (non-renewable energy) increase fine particulate matter (PM<sub>2.5</sub>) emissions (Luo et al. 2021).

It is well known that PM<sub>2.5</sub> mainly comes from human activities and has the characteristics of small particle size, high toxicity, and long atmospheric residence time. In addition, it easily enters the human body through breathing and enters the blood circulation, via which it can endanger the health of various organ systems (Cheng et al. 2020; Zeng et al. 2022), especially the cardiovascular and respiratory systems (Li et al. 2020; Huang et al. 2021; Jia et al. 2022). According to joint research by Yale University, Columbia University, and the World Economic Forum (Wu et al. 2020), China ranked fourth from the bottom in the 2018 Environmental Performance Index, an assessment of environmental quality involving PM<sub>2.5</sub>; the concentration of PM<sub>2.5</sub> in China often far exceeds the WHO Interim Target-1 (IT-1) (Xu et al. 2017). The average life expectancy of residents in northern China is estimated to be 5.5 years lower than that in southern China, mainly due to the increased mortality from cardiopulmonary diseases due to PM<sub>2.5</sub> exposure (Xu et al. 2017). In addition, once the ozone (O<sub>3</sub>) concentration is exceeded, it becomes a primary air pollutant, which is mainly formed by complex photochemical interactions triggered by sunlight and nitrogen oxides (NO<sub>x</sub>) (Khomsi et al. 2022). According to the 2015 Global Burden of Disease Study, O<sub>3</sub> ranked 33rd among the risk factors for premature death and is a major contributor to 254,000 deaths worldwide (Hakim et al. 2019). Long-term exposure to high O<sub>3</sub> concentrations can also damage the human respiratory system, leading to a range of eye diseases (Wang et al. 2022).

Since the Chinese government implemented the Ten Measures for Prevention and Control of Air Pollution in 2013, the air pollution level has slightly decreased, but the situation remains critical (Gu et al. 2019). In recent years, relevant research has mostly focused on the correlation between air pollution and meteorological factors as well as human health in economically developed regions, such as mitigation approaches for residential air pollution emissions in the Beijing-Tianjin-Hebei region (Liu et al. 2019), the relationship between PM<sub>2.5</sub> and meteorological factors in China at seasonal and regional scales (Yang et al. 2017), and the latest meta-analysis to explore the inhomogeneous effects of season, spatial scale, and latitude on the relationship between meteorological factors and COVID-19 propagation (Li et al. 2022a). However, only a few studies have been conducted on cities in less economically developed areas, such as arid and semi-arid regions in northwestern China (Sheng et al. 2018). Urumqi is the

second Eurasian Continental Bridge, bridgehead in northwest China and an important gateway for China's opening to the west (Sheng et al. 2018), but its air pollution is particularly serious, ranking among the top ten most polluted cities in China (Meng et al. 2019). Since 1998, Urumqi has implemented the "Blue Sky Project" with the main purpose of combating air pollution. Since 2012, it has adjusted its energy structure and implemented the "coal-to-gas" project, which is the largest and fastest construction project in China. After the continuous monitoring of PM<sub>2.5</sub> since 2014, the research on spatio-temporal variation of air pollutant concentrations in Urumqi has been lacking (Abudumtailifu et al. 2018).

Previous studies on urban air quality by domestic and foreign researchers have focused on economically developed areas, and many studies have aimed to explore the seasonal variation in air pollutants without considering the potential human impact. Therefore, it is particularly important to explore relevant studies involving urban air pollution and its human health impacts in Urumqi, an arid oasis city. We used the daily average data of major air pollutant levels (PM<sub>2.5</sub>, PM<sub>10</sub>, SO<sub>2</sub>, NO<sub>2</sub>, CO, and O<sub>3-8h</sub>) in Urumqi from 2017 to 2021 to quantitatively analyze the spatiotemporal distribution characteristics of each pollutant, briefly study the impact of COVID-19 prevention and control measures on air pollution during the epidemic, and clarify the impact of PM<sub>2.5</sub> and O<sub>3-8h</sub> mass concentration change characteristics and their wavelet coherence (WTC) with the air quality index (AQI), as well as the changes in PM<sub>2.5</sub>, O<sub>3-8h</sub> pollution levels, and potential human health effects. The research findings provide a scientific reference for local air pollution control and management and are of important practical significance for improving air conditions in Urumqi and other arid oasis cities.

## 2 Materials and methods

### 2.1 Study area

Urumqi (86° 37' 33" E-88° 58' 24" E, 42° 45' 32" N-45° 08' 00" N) is located in the hinterland of the Eurasian continent in the arid region of northwest China and is the farthest city from the ocean (Yin et al. 2019). The region has a typical mid-temperate continental climate. The climate is relatively dry, with an average annual precipitation of approximately 250 mm and an average annual temperature of - 7.5 to 6.2 °C. Urumqi is a city that uses fossil fuels such as coal and natural gas as its main energy sources (Li et al. 2022b). At the same time, Urumqi is also a valley-shaped city with a fragile natural ecology, characterized by long winters, long heating periods, high frequency of gusty winds, and an inversion layer, which are

extremely unfavorable for the dilution and diffusion of atmospheric pollutants and make the city prone to more serious air pollution (Abudumutailifu et al. 2018; Li et al. 2015). As a megacity in China, Urumqi has a permanent population of 4,054,369, its total administrative area is approximately 13,800 km<sup>2</sup>, and the urban built-up area reached 521.6 km<sup>2</sup> by 2020 (<http://tjj.xinjiang.gov.cn>).

### 2.2 Data sources

The data for the concentrations ( $\rho$ ) of PM<sub>2.5</sub>, PM<sub>10</sub>, SO<sub>2</sub>, NO<sub>2</sub>, CO, and O<sub>3\_8h</sub> for Urumqi City from January 1, 2017, to December 31, 2021, used in this study were obtained from the Air Quality Historical Data Query website (<http://www.aqistudy.cn/historydata>). Ten air quality monitoring sites providing continuous daily monitoring based on data from Urumqi were selected (Fig. 1 and Table 1), of which the Xinjiang Academy of Agricultural Sciences Farm (S2), Midong District Environmental Protection Bureau (S6), and HongGuang Shan Area (S9) were industrial reference sites to investigate the impact of industry on air quality; the other seven monitoring sites, Railway Bureau, Toll House, No. 31 Middle School, Monitoring Station, Dabancheng District

Environmental Protection Bureau, Great Green Valley, and Xinjiang Normal University New Campus (S1, S3, S4, S5, S7, S8, and S10) were commercial and residential reference sites to explore the impact of commercial development and residential life on air quality.

### 3 Research methods

The AQI was calculated based on the Technical Provisions on Ambient Air Quality Index (for Trial Implementation) (HJ 633-2012) and Ambient Air Quality Standard“ (GB 3095-2012) (Sheng et al. 2018), as detailed below:

$$IAQI_P = \frac{IAQI_{Hi} - IAQI_{L0}}{BP_{Hi} - BP_{L0}} (C_P - BP_{L0}) + IAQI_{L0} \quad (1)$$

where IAQI<sub>P</sub> represents the air quality score of pollution item P, C<sub>P</sub> is the concentration of pollutant item P, BP<sub>Hi</sub> is the upper limit of the corresponding standard concentration, BP<sub>L0</sub> is the lower limit of the corresponding standard concentration, IAQI<sub>Hi</sub> is the air quality subindex corresponding to BP<sub>Hi</sub>, and IAQI<sub>L0</sub> is the air quality subindex corresponding to BP<sub>L0</sub>.

$$AQI = \max\{AQI_1, AQI_2, AQI_3, \dots, AQI_n\} \quad (2)$$

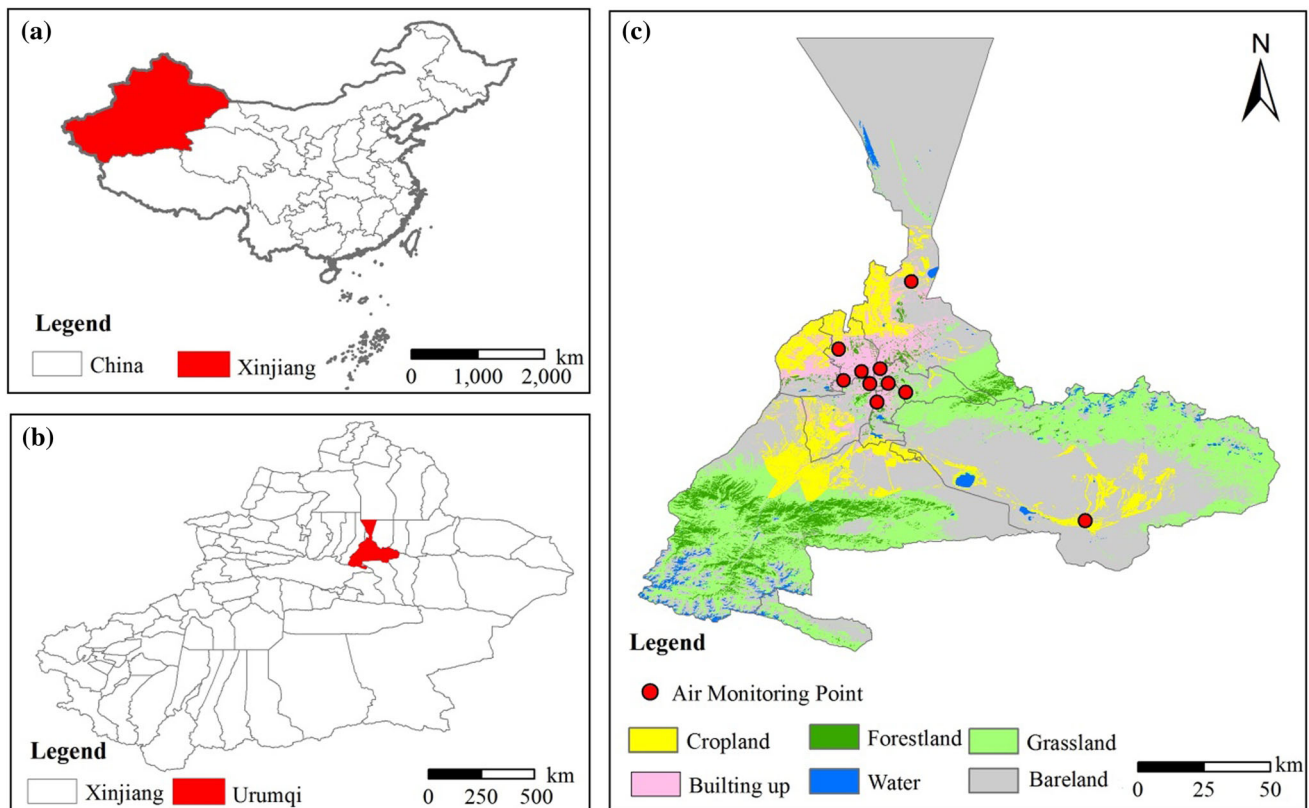


Fig. 1 Schematic map of air quality monitoring sites in the study area

**Table 1** Overview of air quality monitoring stations in Urumqi

Monitoring station	Monitoring station name	District	Distribution	Geographical location	Area type
S1	Railway Bureau	New urban area	City center	43.87°N, 87.55°E	Commercial and residential areas
S2	Xinjiang Academy of Agricultural Sciences Farm	Anning Qu	City fringe	43.94°N, 87.47°E	Industrial area
S3	Toll Collection	Tianshan District	City center	43.76°N, 87.60°E	Commercial and residential areas
S4	No. 31 Middle School	Shuimogou District	City center	43.83°N, 87.64°E	Commercial and residential areas
S5	Monitoring Station	Saybak District	City center	43.83°N, 87.58°E	Commercial and residential areas
S6	Midong District Environmental Protection Bureau	Midong District	City fringe	43.96°N, 87.64°E	Industrial area
S7	Daban City Environmental Protection Bureau	Dabancheng District	City fringe	43.36°N, 88.31°E	Commercial and residential areas
S8	Great Green Valley	Saybak District	City center	43.84°N, 87.69°E	Commercial and residential areas
S9	Hong Guang Shan Area	Midong District	City fringe	43.88°N, 87.61°E	Industrial area
S10	Normal University New Campus	Shuimogou District	City center	43.80°N, 87.70°E	Commercial and residential areas

where IAQI and  $n$  represent the air quality subindex and pollutant item, respectively. As seen from the above formula, if the air quality sub-index of multiple pollutant items exceeds the standard, then the AQI is the one with the largest air quality sub-index of pollutant items.

According to the ambient air quality standard, the air quality monitoring sites in our research area are located in commercial, residential, and industrial zones (Table 2). They all belong to the Class II zone of the ambient air functional area classification. According to the associated requirements, the class II zone applies to secondary concentration limits (Sheng et al. 2018). The 24-h average national secondary standard concentration limits corresponding to each air pollutant  $PM_{2.5}$ ,  $PM_{10}$ ,  $SO_2$ ,  $NO_2$ , and

$CO$  were  $150 \mu\text{g m}^{-3}$ ,  $75 \mu\text{g m}^{-3}$ ,  $150 \mu\text{g m}^{-3}$ ,  $80 \mu\text{g m}^{-3}$ , and  $4 \text{mg m}^{-3}$ , respectively; the national secondary standard for the daily maximum 8-h average concentration limit of  $O_3$  was  $160 \mu\text{g m}^{-3}$ .

According to the AQI levels and the corresponding concentration limits of the  $PM_{2.5}$ , the  $O_3$ \_8h subindex in the Technical Provisions on Ambient Air Quality Index (AQI) (for trial implementation) (HJ 633–2012),  $\rho(PM_{2.5})$ , and  $\rho(O_3\text{-}8\text{h})$  are classified into five levels (Table 2) (Chowdhuri et al. 2022). The higher the ambient air quality index, the higher its level, which indicates more serious pollution and is more detrimental to human health.

**Table 2** Ambient air quality level standards and pollutant concentration limits

Air quality index (AQI)	$\rho(PM_{2.5})$ 24-h average/ $\mu\text{g m}^{-3}$ concentration limit	$\rho(O_3\text{-}8\text{h})$ 8-h average/ $\mu\text{g m}^{-3}$ concentration limit	Air quality index level	Air quality index category	Human Health Response
0–50	0–35	0–100	I	Excellent	Normal activities
51–100	36–75	101–160	II	Good	Affects sensitive people
101–200	76–150	161–265	III	Light pollution	Irritation symptoms appear
201–300	151–250	265–800	IV	Moderately polluted	The heart and respiratory stems affected
> 300	> 250	–	V	Heavy pollution	Reduced tolerance, intense symptoms

### 3.1 Data processing

The original 24-h arithmetic mean of  $\rho(\text{PM}_{2.5})$ ,  $\rho(\text{PM}_{10})$ ,  $\rho(\text{SO}_2)$ ,  $\rho(\text{NO}_2)$ ,  $\rho(\text{CO})$ , and the 8-h arithmetic mean of  $\rho(\text{O}_3)$  from 10 monitoring stations in Urumqi were used in Origin 2021 to generate graphs. At the same time, the means were also used to plot the characteristic curve of the temporal and spatial variation of each pollutant and the proportion of pollutant levels. Differences in  $\text{PM}_{2.5}$  and  $\text{O}_3$ \_8h data between sites and temporal changes within sites were tested using one-way ANOVA (significance level of  $P = 0.05$ ), and all statistical analyses were performed using SPSS statistics 26.0.

Furthermore, we used wavelet coherence analysis to assess AQI,  $\text{PM}_{2.5}$ , and  $\text{O}_3$ \_8h data in Urumqi from 2017 to 2021. Wavelet analysis is a method based on Fourier analysis to display the localized characteristics of the analyzed object from both the time and frequency domains, and is used to study the correlation between two serial data on multiple time scales. Its coefficient can be calculated from the wavelet energy spectrum by using the following equation (Khomsii et al. 2022):

$$R_{YZ}^2(s) = \frac{|\langle W^{YZ}(s) \rangle|^2}{|\langle W^Y(s) \rangle|^2 |\langle W^Z(s) \rangle|^2} \quad (3)$$

$$|W_i^{YZ}(s)| = |W_i^Y(s) \overline{W_i^Z(s)}|$$

where  $Y$  and  $Z$  are the data sequences,  $R_{YZ}^2(s)$  is the wavelet coherence coefficient,  $W_i^{YZ}(s)$  is the wavelet cross-spectrum of the data sequence  $YZ$ ,  $W_i^Y$  and  $W_i^Z$  are the wavelet coefficients of the data sequences  $Y$  and  $Z$ , respectively, and “ $\langle \rangle$ ” is the smooth function of the wavelet energy spectrum. The wavelet toolbox in MATLAB was used for computations.

## 4 Results and discussion

### 4.1 Spatiotemporal variation of air pollutant concentrations and the effect of COVID-19 prevention and control measures

As shown in Fig. 2, the concentrations of  $\text{PM}_{2.5}$ ,  $\text{PM}_{10}$ ,  $\text{SO}_2$ ,  $\text{NO}_2$ , and  $\text{CO}$  in Urumqi showed a “U” shaped cyclical trend from 2017 to 2021, and the trends of  $\text{PM}_{10}$  and  $\text{SO}_2$  were relatively flat compared to those of  $\text{PM}_{2.5}$ ,  $\text{NO}_2$ , and  $\text{CO}$ . Among them, the “U” shaped fluctuation of  $\text{SO}_2$  decreases with time and tends to plateau after April 2019. The national secondary standard for  $\text{SO}_2$  concentration is  $150 \mu\text{g m}^{-3}$ , which is not exceeded at any monitoring sites in Urumqi, and the reason for this is probably because Urumqi is home to a large national

petrochemical and coal chemical base. To reduce air pollution emissions from this energy industry base, the state has adopted other  $\text{SO}_2$  control measures proposed by the Chinese State Council (CSC) Action Plan for Air Pollution Prevention and Control and the Notice on Accelerating the Proposed Small Thermal Power Units Shutdown in China (Wang et al. 2017), thus providing effective control of  $\text{SO}_2$  emissions in this region, so that the  $\text{SO}_2$  concentration is maintained at a low level.  $\text{NO}_2$  fluctuated significantly during low concentration periods (summer and autumn) relative to  $\text{PM}_{2.5}$ , and  $\text{CO}$ , indicating that  $\text{NO}_2$  is more significantly influenced by temperature and solar radiation. The concentrations of  $\text{PM}_{2.5}$ ,  $\text{PM}_{10}$ ,  $\text{SO}_2$ ,  $\text{NO}_2$ , and  $\text{CO}$  showed a small peak from April to September each year, while a high concentration peak occurred from September to March of the following year, showing better air quality in summer and autumn, worse air quality in winter and spring, and pollutant concentration limits exceeding the national secondary standards in winter and spring. The reason for these phenomena may be that coal-fired heating and motor vehicles in winter emit many pollutants, such as sulfur dioxide, nitrogen oxides, particulate matter, and other pollutants. In addition, due to various climate factors such as less precipitation, dry climate, short sunshine time, low wind speed, and a thick temperature inversion layer can be detrimental to the diffusion of air pollutants and seriously affect air quality (Meng et al. 2019). The daily maximum 8-h average concentration of  $\text{O}_3$  showed the opposite trend to the above five pollutants, demonstrating an inverted “V” shape, and its high peak (June–July) and low peak (January) values were found to correspond inversely to the high peak (January) and low peak (June–July) values of  $\text{NO}_2$ . The reason for this phenomenon may be that  $\text{NO}_2$ , as the main precursor of secondary pollutants, is involved in photochemical reactions, while  $\text{O}_3$  is mainly generated due to photochemical reactions of nitrogen oxides ( $\text{NO}_x$ ) and volatile organic compounds (VOCs) in the presence of ultraviolet light. The intensity of solar radiation has an important influence on atmospheric photochemical reactions, and the changes in atmospheric temperature can better reflect changes in the intensity of solar radiation, that is, high temperature and high radiation are favorable for  $\text{O}_3$  generation (Liu and Wang 2020; Lu et al. 2021).

According to the announcement on the website of the Urumqi Municipal People’s Government regarding the prevention and control of the 2019 novel coronavirus (COVID-19) outbreak, the first wave of prevention and control measures ran from January 26, 2020, when the city launched the Level 1 response to major public health emergencies, to March 21, when the response level was lowered to Level 4, coinciding with the Lunar New Year festival. The second wave of prevention and control measures ran from July 20 at the high-risk level, until the risk



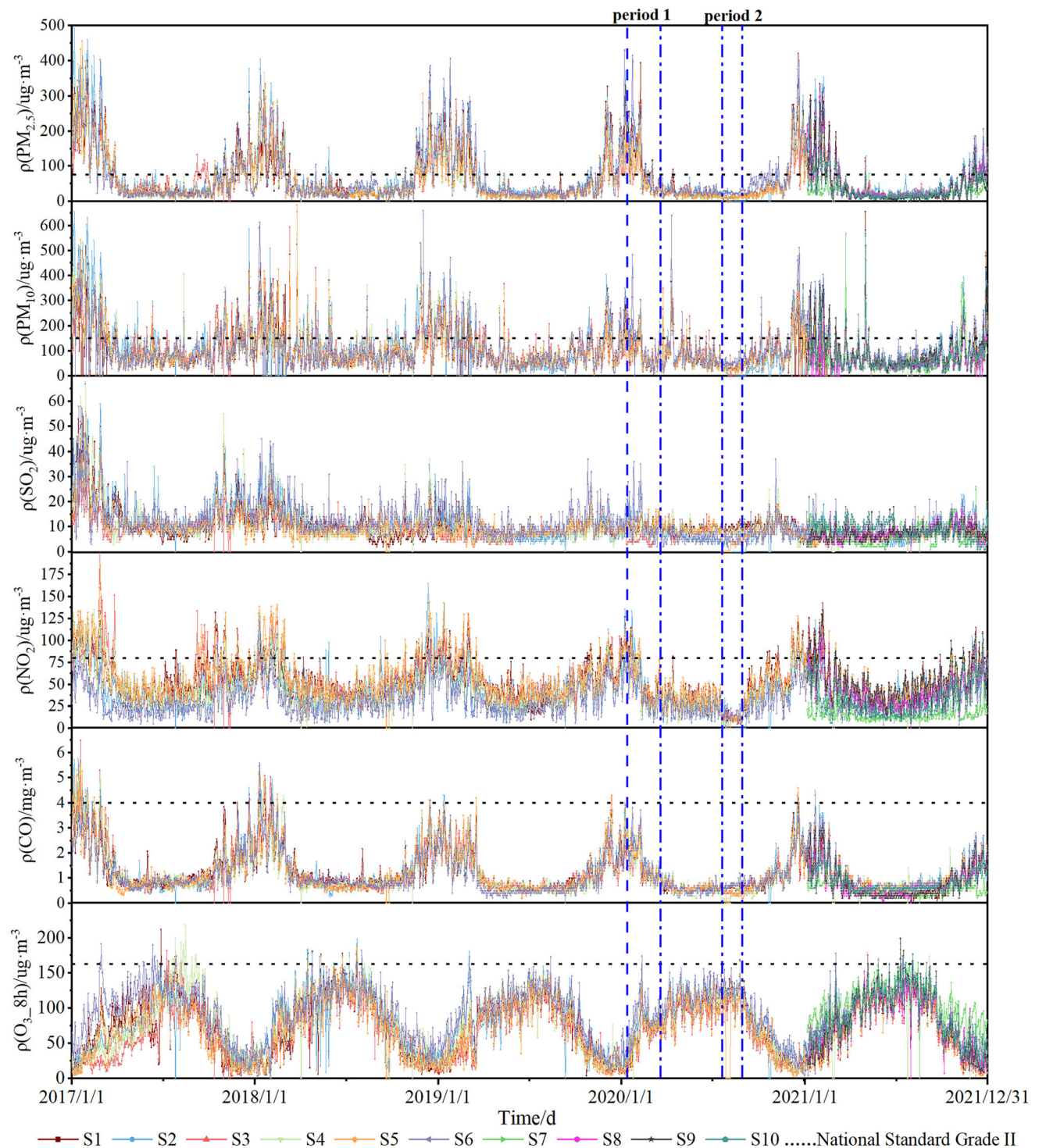


**Fig. 2** Variation trends in air pollutant concentrations in Urumqi from 2017 to 2021 (the blue vertical line is the period of COVID-19 epidemic prevention and control, periods 1 and period 2 are the first and the second blockade period)

level was lowered to low risk on August 29. The periods of 2017–2019 and 2021 were selected and simultaneously analyzed to compare the impact of government prevention and control measures on air pollutants during the COVID-19 outbreak period. The first and second waves of epidemic

prevention and control occurred in the winter and summer, respectively. The concentration of pollutants in Wave 1 was significantly higher than that in Wave 2 (Fig. 2), which is consistent with the trend of pollutant concentrations in previous years. The pollutants  $PM_{2.5}$ ,  $PM_{10}$ ,  $SO_2$ ,  $NO_2$ , and

CO decreased significantly from February 12 to March 21 during the first wave of the study period compared with the same period in 2017–2019 and 2021, and the increase in  $O_3$  was slightly reduced. Similar conclusions were reached by Ravina et al. (2021), who suggested that brief and strict lockdowns would help improve air quality (Das et al. 2021; Kumar et al. 2022). The concentrations of each pollutant also decreased during the second wave of the study period compared to the control period, with significant decreases in  $PM_{10}$  and  $NO_2$ . Industrial production, combustion of fossil fuels such as oil and coal, and vehicle exhaust from motor vehicle travel are the main anthropogenic sources of particulate matter and  $NO_x$  generation (Zhang et al. 2021; Ambade et al. 2021a, b). During COVID-19, home isolation and reduction of human activities can effectively reduce the concentration of air pollutants (Naqvi et al. 2022). The decreases in  $PM_{10}$  and  $NO_2$  concentrations suggest that the government's strict traffic controls, restrictions on people's movement, suspension of industrial and commercial production activities, delaying schooling, and other measures during the outbreak, played an important role in reducing the concentration of air pollutants.

#### 4.2 Spatiotemporal variation in $\rho(PM_{2.5})$ and $\rho(O_3_{8h})$ at six monitoring sites

Owing to rapid socioeconomic development, expansion of urbanization, and increased consumption of coal resources, the particulate matter content in the air is increasing, and the pollution problem of  $O_3$  is becoming more prominent, resulting in a significant decrease in the quality of the atmospheric environment. Therefore, this study focuses on the spatiotemporal variation characteristics of  $PM_{2.5}$ , and  $O_3_{8h}$  from 2017 to 2021. As shown in Table 3, the average values of  $\rho(PM_{2.5})$  at the six monitoring sites in Urumqi from 2017 to 2021 were 78.93, 63.64, 60.13, 56.54, and 50.18  $\mu g m^{-3}$ , respectively, showing a decrease each year. The maximum value (97.95  $\mu g m^{-3}$ ) occurred at site S2 in 2017 and the lowest value (40.77  $\mu g m^{-3}$ ) occurred at site S3 in 2021. In addition, the values measured at sites S1, S2, S3, S4, and S5 were significantly different ( $P < 0.05$ ) between 2017 and 2018–2021, whereas differences between years at site S6 were not significant. The variability between monitoring sites indicated less significant differences between monitoring sites S2 and S6, but the difference with the other four sites was more significant. The highest value of  $\rho(O_3_{8h})$ , 96.39  $\mu g m^{-3}$ , occurred at site S6 in 2017, the lowest value (54.61  $\mu g m^{-3}$ ) occurred at site S3 in 2017, and the average value from 2017 to 2021 showed a trend that increased, then decreased, and then increased. Among the values, the differences between years within sites S1 and S6 were

insignificant, whereas the differences between different monitoring sites in the same year were significant, especially between 2017 and 2019. Regarding the distribution area, the measurements of  $\rho(PM_{2.5})$  and  $\rho(O_3_{8h})$  from 2017 to 2021 in Urumqi were higher at sites S2 and S6 than at the other four sites, which may be because the sites S2 and S6 are industrial areas and the other four sites are commercial and residential areas. As industrial production consumes a large amount of fossil fuels and other energy sources, the emission of various air pollutants increases (Fang and Yu 2021; Wen et al. 2022; Ambade et al. 2022), resulting in more severe air pollution at those two stations.

#### 4.3 Wavelet-based analysis of the correlation between AQI and $\rho(PM_{2.5})$ and $\rho(O_3_{8h})$

This aim of this part of our study was to explore the correlation between AQI, and  $PM_{2.5}$  and  $O_3_{8h}$  using the wavelet coherence method. The time scale is provided on the horizontal axis, whereas the frequency scale is represented on the vertical axis (Ghazani et al. 2022). The frequency range spans high frequency (0–16), medium frequency (16–128) and low frequency (128–512), and we used color coding (blue to red, low to high) to define the coherent wavelet spectral intensity (Cheng et al. 2021; Fareed et al. 2021). The cones of influence represent colored regions unaffected by wavelet spectral edge effects, and the range enclosed by the thick line represents 95% confidence relative to red noise (Habib et al. 2021; Hung 2022).

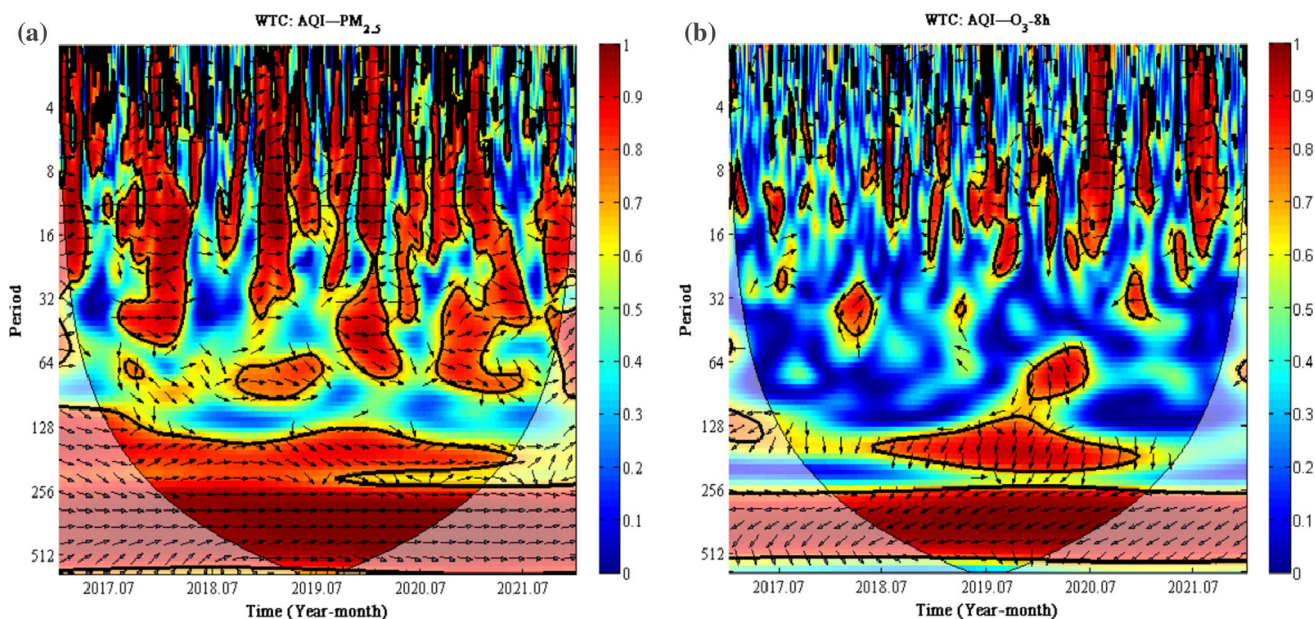
Furthermore, the arrows in the wavelet coherence diagram indicate the process of interconnection and causality between AQI,  $PM_{2.5}$ , and  $O_3_{8h}$ . Arrows pointing to the right ( $\rightarrow$ ) (in-phase) and left ( $\leftarrow$ ) (out-of-phase) indicate the positive and negative correlations, respectively. The up ( $\uparrow$ ) and down ( $\downarrow$ ) arrows indicate that there is a leading and lagging relationship between the two factors, respectively (Ghazani et al. 2022).

Figure 3a shows the WTC between AQI and  $PM_{2.5}$  at site S1. The AQI and  $PM_{2.5}$  sequences at the S1 site are in phase, and there is a strong (positive) relationship between the two variables. Furthermore, when we focus on the direction of the sign (to the right), we can infer that the two variables were positively correlated throughout the study period. Furthermore, we found strong correlations between the data series of the two variables throughout the study period, mainly in the range of 0–80 (mid-high frequency) and 128–512 (low frequency). Figure 3b shows the WTC between AQI and  $O_3_{8h}$  at S1. The linkage between AQI and  $O_3_{8h}$  is in the range of 0–16 (high frequency) and 128–512 (low frequency) from 2018–2021. This association was stronger at low frequencies. The down and left

**Table 3** Changes in  $\rho(\text{PM}_{2.5})$  and  $\rho(\text{O}_3\text{-8h})$  at different monitoring sites in Urumqi from 2017 to 2021

Project	2017	2018	2019	2020	2021	Annual mean
$\rho(\text{PM}_{2.5})/\mu\text{g m}^{-3}$						
S1	81.54 ± 4.34Ab	60.13 ± 3.21Bbc	61.72 ± 3.61Bb	59.11 ± 3.94Bb	53.07 ± 3.22Bab	63.11 ± 1.66
S2	97.95 ± 5.36Aa	76.73 ± 3.92Ba	72.77 ± 3.75BCa	63.45 ± 3.96Cab	61.00 ± 3.37Ca	74.37 ± 1.87
S3	72.59 ± 3.50Ab	57.84 ± 2.89Bc	52.90 ± 2.71BCbc	48.15 ± 3.35CDc	40.77 ± 1.80Dc	54.45 ± 1.24
S4	73.87 ± 4.17Ab	59.85 ± 3.29Bbc	49.56 ± 2.69Cc	46.44 ± 2.98Cc	43.37 ± 2.45Cc	54.61 ± 1.44
S5	75.97 ± 4.27Ab	57.58 ± 3.21Bc	52.15 ± 2.99BCbc	48.93 ± 3.20BCc	45.23 ± 2.75Cbc	55.97 ± 1.51
S6	71.67 ± 4.37Ab	69.72 ± 4.04Ab	71.71 ± 4.11Aa	73.21 ± 4.25Aa	57.68 ± 3.58Ba	68.70 ± 1.83
Mean	79.65 ± 1.79	63.64 ± 1.41	60.13 ± 1.38	56.54 ± 1.45	50.18 ± 1.20	–
$\rho(\text{O}_3\text{-8h})/\mu\text{g m}^{-3}$						
S1	71.60 ± 2.13Ab	76.55 ± 2.45Acd	71.99 ± 2.07Ac	77.24 ± 2.03Ab	76.24 ± 2.08Abc	74.72 ± 0.97
S2	68.11 ± 1.89Cbc	88.6 ± 2.41Aab	81.77 ± 2.01Bb	68.45 ± 2.25Cc	87.89 ± 2.06Aa	78.85 ± 0.98
S3	54.61 ± 2.02Cd	72.27 ± 2.09Ad	65.62 ± 1.96Bd	68.19 ± 1.77BCc	73.78 ± 1.83Ac	66.90 ± 0.88
S4	73.19 ± 2.36Bb	82.61 ± 2.28Abc	74.71 ± 2.16Bc	78.99 ± 1.98ABb	81.34 ± 2.14Ab	78.17 ± 0.98
S5	63.70 ± 2.06Cc	76.61 ± 2.41Acd	70.09 ± 2.14ABcd	68.59 ± 2.02BCc	75.53 ± 2.23Abc	71.07 ± 0.98
S6	96.39 ± 2.13Aa	90.26 ± 2.02Ba	90.39 ± 1.99Ba	92.22 ± 1.94ABa	89.75 ± 1.98Ba	91.80 ± 0.90
Mean	71.26 ± 0.90	81.15 ± 0.94	75.76 ± 0.86	75.61 ± 0.84	80.75 ± 0.85	–

Mean ± standard error, different capital letters indicate statistically significant differences between study years, and lowercase letters indicate statistically significant differences between monitoring sites ( $P < 0.05$ ). No analysis was included because of missing data from monitoring sites S7, S8, S9, and S10

**Fig. 3** Wavelet coherence of AQI at site S1 with  $\text{PM}_{2.5}$  (a) and  $\text{O}_3\text{-8h}$  (b)

arrows indicate that AQI drives the increase in  $\text{O}_3\text{-8h}$  concentration with a negative sign.

Figure 4a shows the WTC between AQI and  $\text{PM}_{2.5}$  at site S2. It can be concluded that there is a strong relationship (positive correlation) between AQI and  $\text{PM}_{2.5}$  at site S2 throughout the study period. Furthermore, it showed high power at ratios of 0–50 and 100–512 throughout the

period, suggesting that AQI significantly affected the concentration changes of  $\text{PM}_{2.5}$ . Figure 4b shows the WTC between AQI and  $\text{O}_3\text{-8h}$  at S2. The linkage between these two variables was mainly reflected in the range of 0–25 (high frequency) in 2019–2021 and 256–512 (low frequency) in 2018–2020. Looking at the direction of the arrows, we found that AQI and  $\text{O}_3\text{-8h}$  were positively



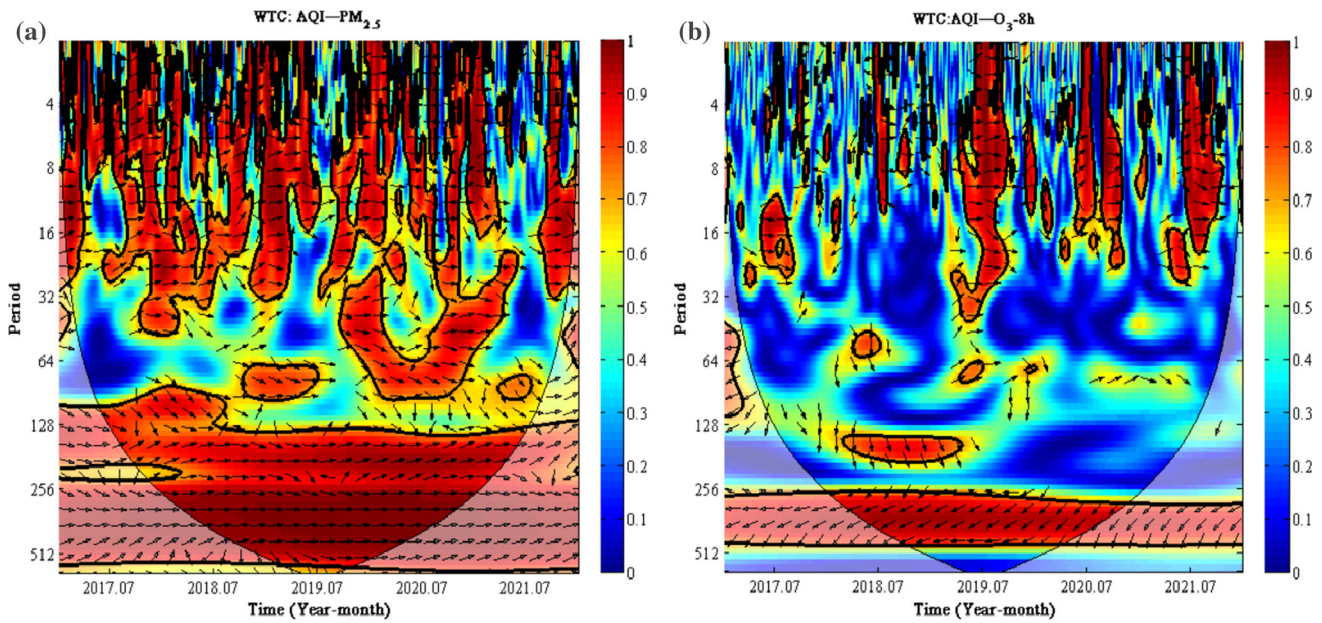


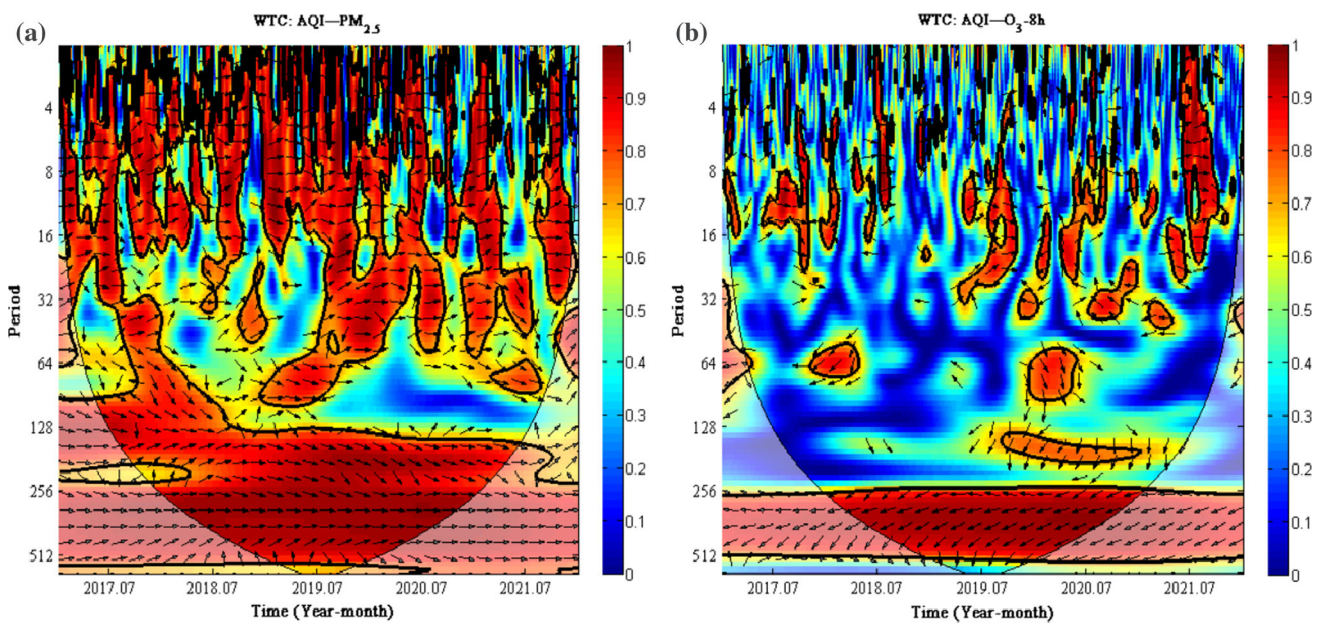
**Fig. 4** Wavelet coherence of AQI at site S2 with  $PM_{2.5}$  (a) and  $O_3_{8h}$  (b)

correlated with  $O_3_{8h}$  at high wavelet power (right), but negatively correlated at low wavelet power, with  $O_3_{8h}$  lagging behind AQI (bottom left).

Figure 5a shows the WTC between AQI and  $PM_{2.5}$  at site S3. The results showed that AQI at site S3 had a positive correlation with  $PM_{2.5}$  in all periods, suggesting that the fluctuation of  $PM_{2.5}$  could be well expressed by AQI. Figure 5b shows the WTC between the AQI and  $O_3_{8h}$  at S3. We can observe a linkage between AQI and

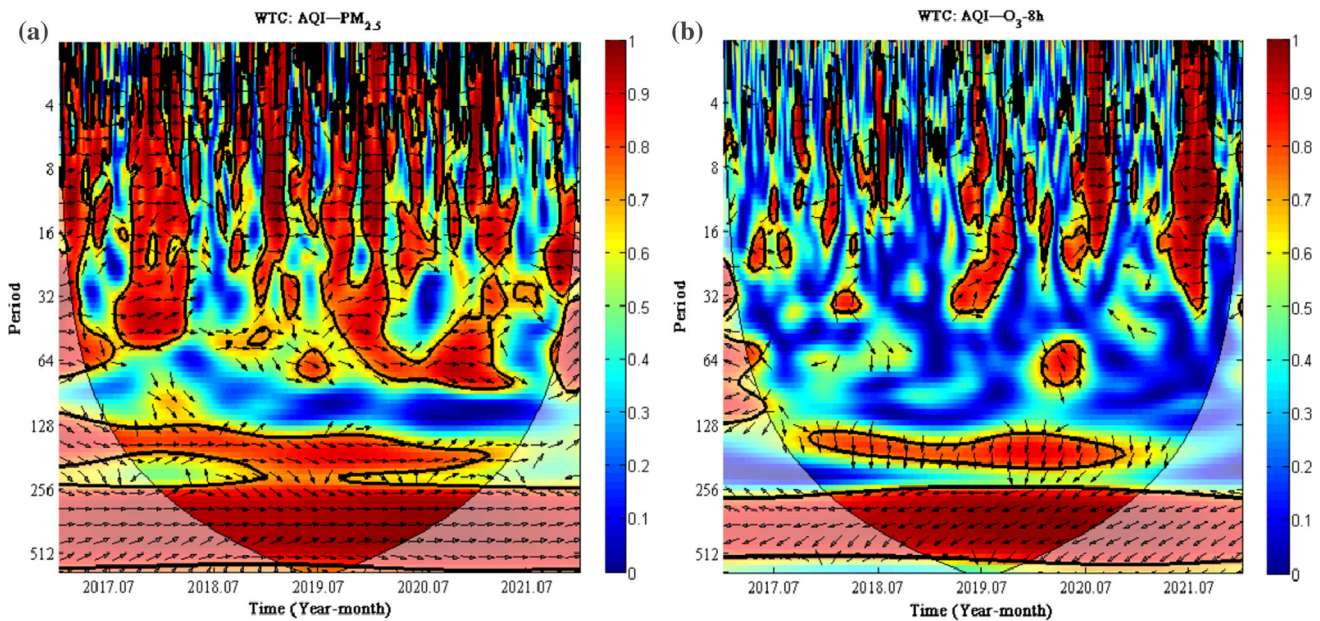
$O_3_{8h}$  in the range of 256–512 (low frequency) in 2018–2020. In addition, the downward and left arrows indicate that  $O_3_{8h}$  lagged the AQI data series, and there was a negative correlation between AQI and  $O_3_{8h}$ .

Figure 6a shows the WTC between AQI and  $PM_{2.5}$  at site S4. It can be seen from Fig. 6a that the AQI of site S4 is in the same phase as  $PM_{2.5}$  (positive correlation), and the linkage between the two is in the mid-to-high frequency range of 0–64 in 2017–2021 and 128–512 low-frequency



**Fig. 5** Wavelet coherence of AQI at site S3 with  $PM_{2.5}$  (a) and  $O_3_{8h}$  (b)



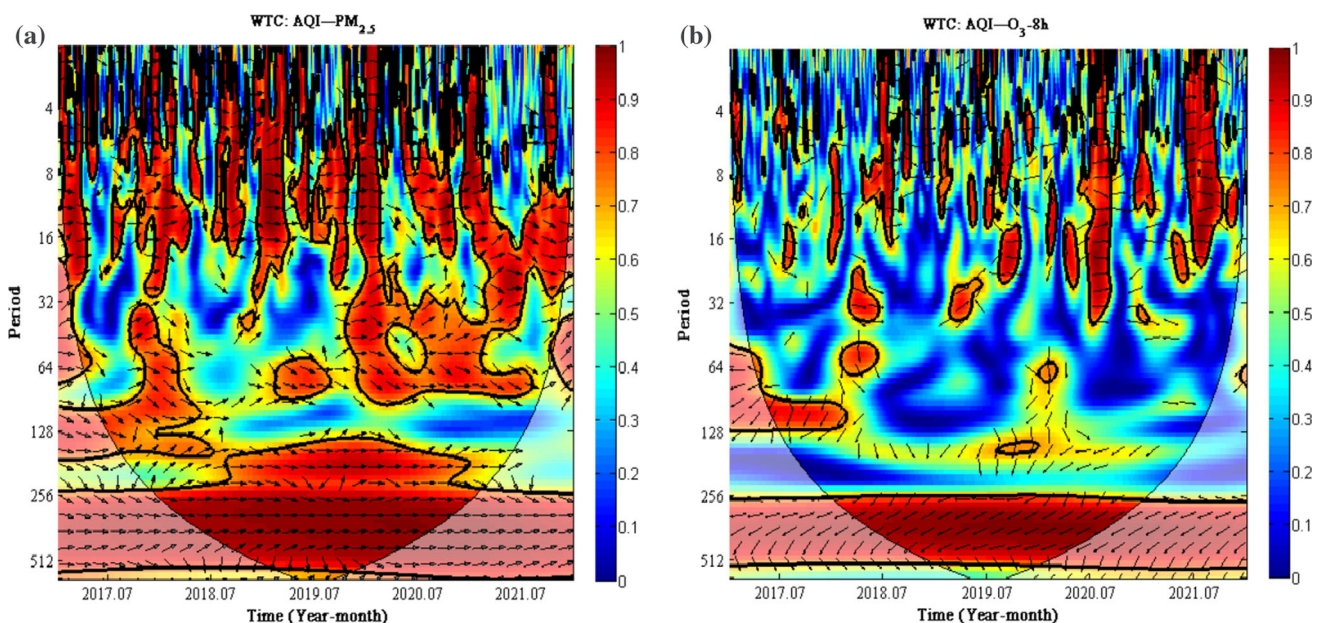


**Fig. 6** Wavelet coherence of AQI at site S4 with PM<sub>2.5</sub> (a) and O<sub>3-8h</sub> (b)

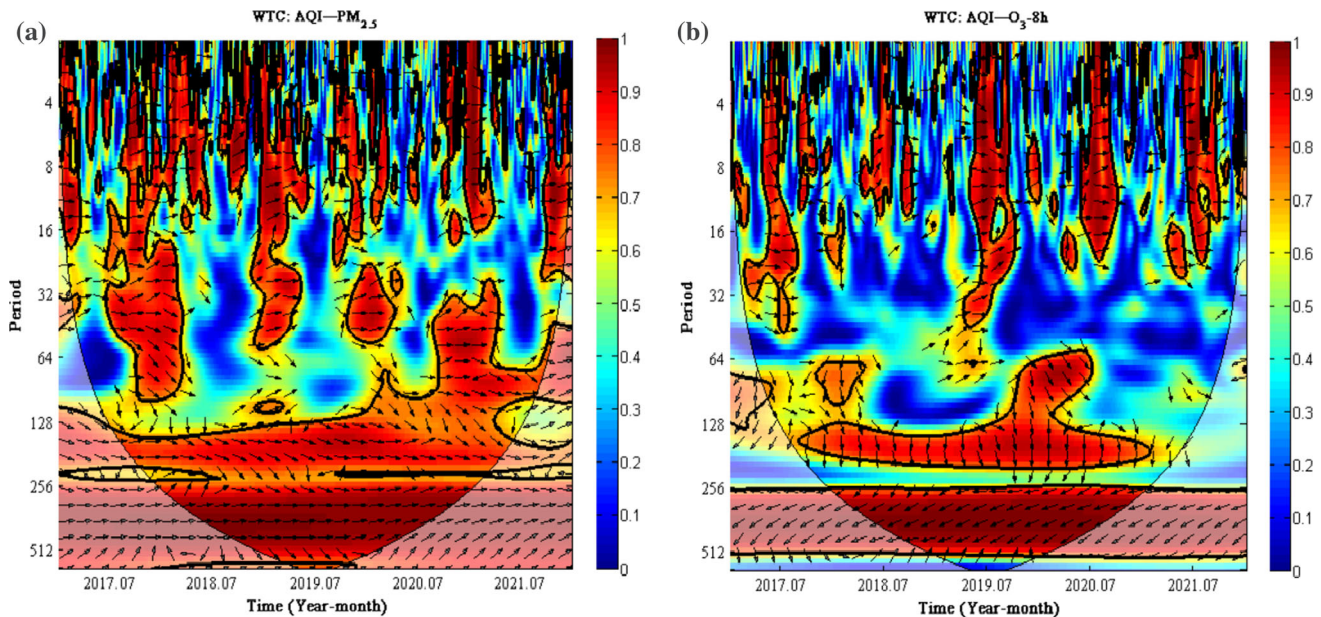
range in 2018–2021. Figure 6b shows the WTC between the AQI and O<sub>3-8h</sub> at S4. The linkage between AQI and O<sub>3-8h</sub> showed a negative correlation in the high-frequency range of 0–32 in 2019, 2020, and 2021, and the low-frequency range of 128–200 and 256–512 in 2018–2020. In addition, the O<sub>3-8h</sub> data series had a certain lag relative to the AQI.

Figure 7a shows the WTC between AQI and PM<sub>2.5</sub> at site S5. We observed a strong (positive) relationship

between the S5 site AQI and PM<sub>2.5</sub>. Additionally, when we focus on the direction of the sign, we can infer that the two variables are positively correlated across all periods. Furthermore, this strong correlation was observed throughout the study period with all ranges (high, mid, and low-frequency scales). Figure 7b shows the WTC between AQI and O<sub>3-8h</sub> at S5. There is a strong (negative) relationship between AQI and O<sub>3-8h</sub> in the high-frequency range of 0–32 in 2020 and 2021, the 64–128 (mid frequency) range



**Fig. 7** Wavelet coherence of AQI at site S5 with PM<sub>2.5</sub> (a) and O<sub>3-8h</sub> (b)



**Fig. 8** Wavelet coherence of AQI at site S6 with  $PM_{2.5}$  (a) and  $O_3_{8h}$  (b)

in 2017–2018, and the low-frequency range of 256–512 in 2018–2020. This association was stronger at low frequencies.

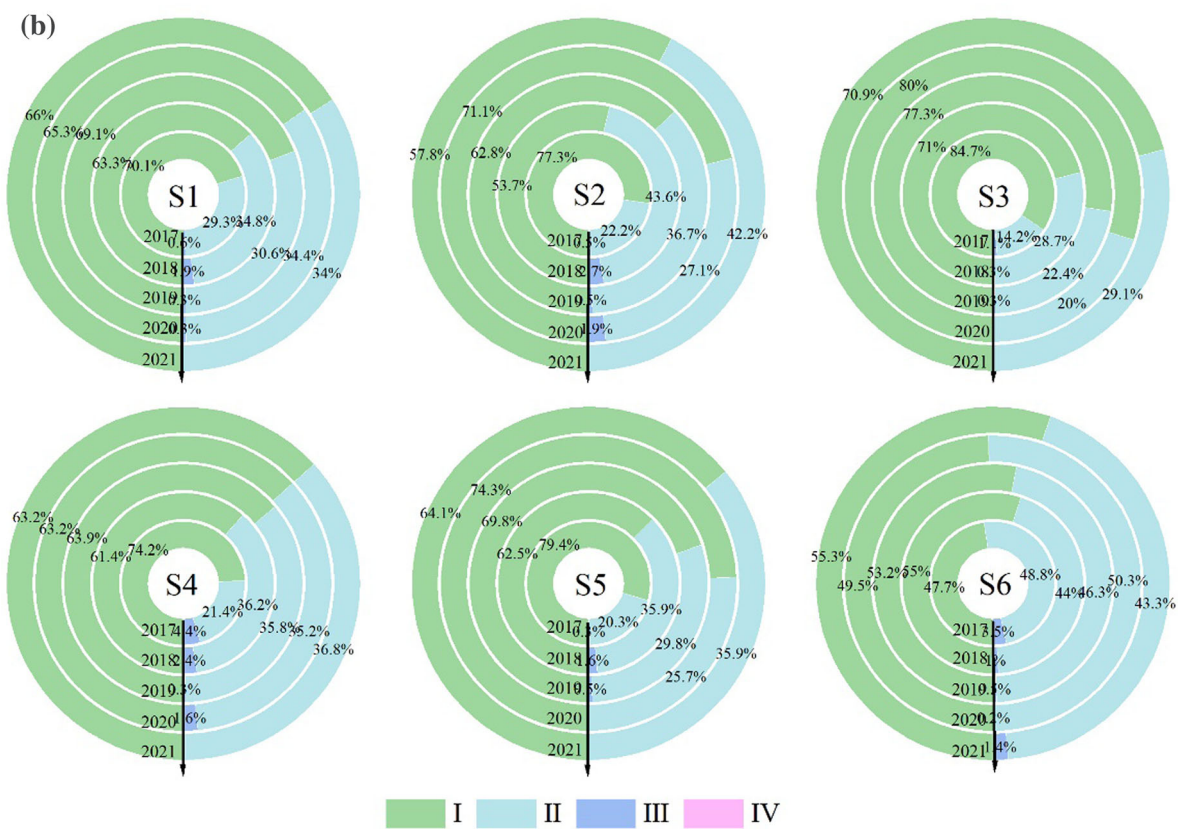
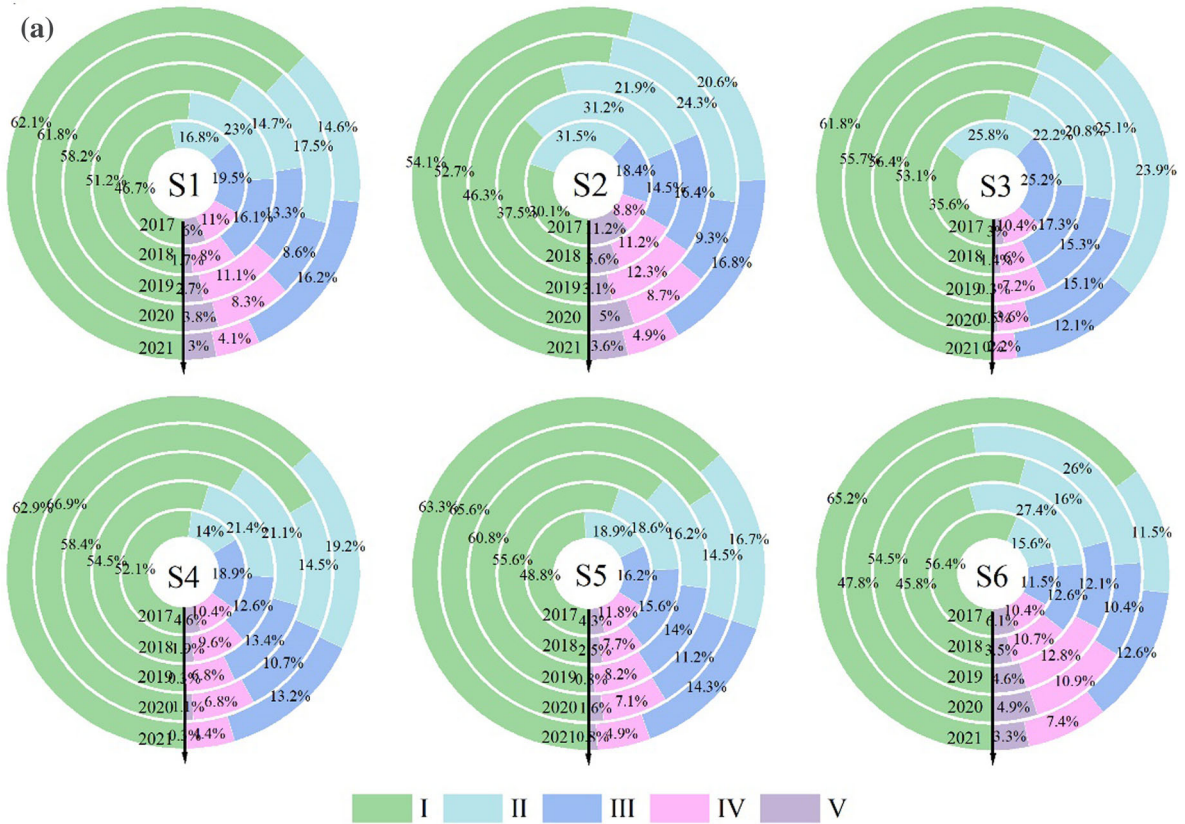
Figure 8a shows the WTC between AQI and  $PM_{2.5}$  at site S6. There was a strong (positive) relationship between AQI and  $PM_{2.5}$  at site S6 in all periods; however, the linkage between the two was stronger in the low-frequency range (128–512). Meanwhile, the downward and right arrows indicate that AQI has a positive effect on  $PM_{2.5}$ . Figure 8b shows the WTC between AQI and  $O_3_{8h}$  at S6. The strong linkage between AQI and  $O_3_{8h}$  is mainly reflected in the 64–128 (mid frequency) and 256–512 (low frequency) ranges from 2018–2020. We carefully observe the arrow directions; the downward and left arrow directions indicate that the data series of  $O_3_{8h}$  lags the AQI, and there is a negative correlation between the two.

As the above wavelet coherence analysis results show, the AQI of each station had continuous wavelet coherence with  $PM_{2.5}$  and  $O_3_{8h}$  at different periods and demonstrated the same or opposite phase, indicating that there was a significant correlation between AQI,  $PM_{2.5}$ , and  $O_3_{8h}$ . Moreover, the AQI data series describes fluctuations in  $PM_{2.5}$ . This result implies that in the future, the AQI data series can be used to explore the study of  $PM_{2.5}$ , in different periods and frequency domains for a long time and provide reliable data support for the management of air pollution and assessment of health risks in the region.

#### 4.4 Air pollution levels of $\rho(PM_{2.5})$ and $\rho(O_3_{8h})$ and potential effects on human health

As shown in Table 2 and Fig. 9a, from 2017 to 2021, the proportion of days with  $PM_{2.5}$  air quality at the S3, S4, and S5 monitoring points in Urumqi City graded I (excellent) and grade II (good) increased year by year, indicating that the air qualities in these three areas tend to be good, and the conditions are more habitable. Sites S1, S2, and S6 showed a trend of first increasing, then decreasing, and finally increasing again. Moreover, the total number of days graded as IV (moderate pollution) and V (severe pollution) at sites S1, S2, and S6 accounted for approximately 15% of the total days, which was twice the proportion of higher air pollution days at sites S3, S4, and S5. This may be attributed to the fact that site S1 is located in the center of Urumqi City, with a dense population, increased use of fossil fuels such as oil and coal for residential life, and frequent motor vehicle trips, resulting in poor air quality in the region (Zhang et al. 2021). In contrast, sites S2 and S6 are located in industrial areas, where industrial production requires a large amount of energy, leading to increased emissions of air pollutants and poor air quality (Ambade et al. 2020; Pei et al. 2021; Wen et al. 2022). High concentrations of  $PM_{2.5}$ , are likely to increase resident morbidity, hospitalization, and mortality due to respiratory diseases, cardiovascular diseases, and cancer (Zhang et al. 2000). Overall, the total number of days with excellent and good grades accounted for 80% of the year 2021 at the six monitoring sites. Compared to 2017, the number of days with excellent and good grades increased significantly, and







◀ **Fig. 9** Percentage of days with PM<sub>2.5</sub> (a) and O<sub>3</sub>-8h (b) pollution levels at 6 monitoring sites in Urumqi

the number of days with moderate and heavy pollution decreased significantly by 2021. The proportion of heavily polluted days decreased to 0%–0.3% at sites S3, S4, and S5. From Table 2 and Fig. 9b, the percentage of days with O<sub>3</sub>-8h air quality at sites S1, S3, S5, and S6, classified as I and II, showed a trend of increasing and then decreasing, but the number of excellent and good days accounted for more than 90% of the total number of days in a year. The percentage of Class III days at sites S2, S4, and S6 was slightly larger than that at the other three sites, and the pollution was more severe, which can lead to irritated eyes and respiratory system of high-risk people living at these three sites and uncomfortable living conditions (Zhang et al. 2019).

Based on Fig. 9, we found that the pollution levels of PM<sub>2.5</sub> and O<sub>3</sub>-8h at sites S2 and S6 were significantly greater than those at several other sites, probably because this air quality monitoring site is located in the industrial development area of Urumqi City, where industrial emissions of volatile organic compounds (VOCs) and motor vehicle movements cause an increase in the concentrations of PM<sub>2.5</sub> and O<sub>3</sub>-8h in the air (Bian et al. 2019), causing air pollution and posing certain health risks to the residents living and moving around the site; therefore, it should be of concern to the relevant authorities.

## 5 Conclusion

The concentrations of PM<sub>2.5</sub>, PM<sub>10</sub>, SO<sub>2</sub>, NO<sub>2</sub>, and CO among the six air pollutants at 10 air monitoring stations in Urumqi during 2017–2021 showed a cyclical trend of low concentrations in summer and autumn, and high concentrations in winter and spring, while the concentration of O<sub>3</sub> showed the opposite trend. The “valley-shaped” urban characteristics of Urumqi and the residents’ long heating period in winter have certain contributions to the high concentration of air pollutants in winter and spring. In addition, the ANOVA results for PM<sub>2.5</sub> and O<sub>3</sub>-8h show that air pollution is more serious in industrial areas than in commercial and residential areas, and that the rapid industrialization of the city has exacerbated air pollution to some extent, threatening the health of urban residents in the area. Therefore, relevant departments should take effective measures to control air pollutant emissions from industrial areas to improve the overall air pollution situation in the city and protect the health of urban residents. Furthermore,

the concentrations of each pollutant decreased during the brief blockade period during COVID-19, suggesting that the apparent positive results on air quality during the COVID-19 blockade period can serve as a basis for government and regulatory agencies to argue that stringent air quality policies can significantly improve the environment and human health.

This study may enrich the gap in the scientific research on air pollution in arid oasis city. However, systematic studies on the interactions between air pollutants and COVID-19 (whether blockades during COVID-19 reduce air pollution and whether increases in air pollutants have an impact on virus transmission and human health threats) are lacking and need to be refined in future research. Finally, in the next few years, urban planners in Urumqi should take actions such as reducing traffic congestion, guaranteeing one day less driving per week, and strict regulations on toxic industries to reduce emissions of major air pollutants to control air pollution in targeted urban areas.

**Acknowledgements** The authors would like to express their sincere gratitude to the Air Quality Historical Data Query website for sharing the air quality data processed in our paper. We thank Dr. Shi Lei for cartography of the map of the study area (Fig. 1). We would also like to express our thanks to the editor and anonymous reviewers for providing valuable and constructive comments that greatly helped us improve our manuscript.

**Author contributions** TA: conceptualization, methodology, validation, formal analysis, data curation, investigation, writing – review and editing, and supervision. YXS and TA: Data collection, analysis, and writing of the original draft. ÜH, FB, RR: Editing and review. All authors have read and approved the final manuscript.

**Funding** This research was supported by the National Natural Science Foundation of China (NSFC project No: 32160367) and the China Postdoctoral Science Foundation (No. 2021M6908).

**Data availability** Data may be obtained from the authors upon reasonable request.

## Declarations

**Conflict of interest** The authors declare no competing interests.

## References

- Abudumutailifu M, Halik U, Aishan T, Keyimu M, Nasirdin N, Ainiwaer A (2018) Variation characteristics of the main atmospheric pollutant concentration in Urumqi. *Ecol Environ Sci* 27(3):533–541. <https://doi.org/10.16258/j.cnki.1674-5906.2018.03.018>
- Almetwally A, Bin-Jumah M, Allam A (2020) Ambient air pollution and its influence on human health and welfare: an overview. *Environ Sci Pollut Res* 27(20):24815–24830. <https://doi.org/10.1007/s11356-020-09042-2>
- Ambade B, Sankar TK, Kumar A, Sethi SS (2020) Characterization of PAHs and n-alkanes in atmospheric aerosol of Jamshedpur City.

- India J Hazard Toxic Radio 24(2):04020003. [https://doi.org/10.1061/\(ASCE\)JHZ.2153-5515.0000490](https://doi.org/10.1061/(ASCE)JHZ.2153-5515.0000490)
- Ambade B, Sankar TK, Kumar A, Gautam AS, Gautam S (2021a) COVID-19 lockdowns reduce the Black carbon and polycyclic aromatic hydrocarbons of the Asian atmosphere: source apportionment and health hazard evaluation. *Environ Dev Sustain* 23(8):12252–12271. <https://doi.org/10.1007/s10668-020-01167-1>
- Ambade B, Kumar A, Sahu LK (2021b) Characterization and health risk assessment of particulate bound polycyclic aromatic hydrocarbons (PAHs) in indoor and outdoor atmosphere of Central East India. *Environ Sci Pollut R* 28(40):56269–56280. <https://doi.org/10.1007/s11356-021-14606-x>
- Ambade B, Kumar A, Kumar A, Sahu LK (2022) Temporal variability of atmospheric particulate-bound polycyclic aromatic hydrocarbons (PAHs) over central east India: sources and carcinogenic risk assessment. *Air Qual, Atmos Hlth* 15(1):115–130. <https://doi.org/10.1007/s11869-021-01089-5>
- Bian Y, Huang Z, Ou J, Zhong Z, Xu Y, Zhang Z, Xiao X, Ye X, Wu Y, Yin X, Li C, Chen L, Shao M, Zheng J (2019) Evolution of anthropogenic air pollutant emissions in Guangdong Province, China, from 2006 to 2015. *Atmos Chem Phys* 19(18):11701–11719. <https://doi.org/10.5194/acp-19-11701-2019>
- Chen F, Chen Z (2021) Cost of economic growth: air pollution and health expenditure. *Sci Total Environ*. <https://doi.org/10.1016/j.scitotenv.2020.142543>
- Cheng L, Zhang T, Chen L, Li L, Wang S, Hu S, Yuan L, Wang J, Wen M (2020) Investigating the impacts of urbanization on PM2.5 pollution in the Yangtze River Delta of China: a spatial panel data approach. *Atmosphere*. <https://doi.org/10.3390/atmos11101058>
- Cheng V, Saber A, Arnillas C, Javed A, Richards A, Arhonditsis G (2021) Effects of hydrological forcing on short- and long-term water level fluctuations in Lake Huron-Michigan: a continuous wavelet analysis. *J Hydrol*. <https://doi.org/10.1016/j.jhydrol.2021.127164>
- Chowdhuri I, Pal S, Arabameri A, Arabameri A, Ngo PTT, Roy P, Saha A, Ghosh M, Chakraborty R (2022) Have any effect of COVID-19 lockdown on environmental sustainability? A study from most polluted metropolitan area of India. *Stoch Env Res Risk A* 36(1):283–295. <https://doi.org/10.1007/s00477-021-02019-8>
- Das M, Das A, Sarkar R, Saha S, Mandal A (2021) Examining the impact of lockdown (due to COVID-19) on ambient aerosols (PM2.5): a study on Indo-Gangetic Plain (IGP) Cities, India. *Stoch Env Res Risk A* 35(6):1301–1317. <https://doi.org/10.1007/s00477-020-01905-x>
- Du Y, Sun T, Peng J, Fang K, Liu Y, Yang Y, Wang Y (2018) Direct and spillover effects of urbanization on PM2.5 concentrations in China's top three urban agglomerations. *J Clean Prod* 190:72–83. <https://doi.org/10.1016/j.jclepro.2018.03.290>
- Du Y, Wan Q, Liu H, Liu H, Kapsar K, Peng J (2019) How does urbanization influence PM2.5 concentrations? Perspective of spillover effect of multi-dimensional urbanization impact. *J Clean Prod* 220:974–983. <https://doi.org/10.1016/j.jclepro.2019.02.222>
- Fang D, Yu B (2021) Driving mechanism and decoupling effect of PM2.5 emissions: empirical evidence from China's industrial sector. *Energy Policy* 149:1. <https://doi.org/10.1016/j.enpol.2020.112017>
- Fareed Z, Bashir M, Bilal SS (2021) Investigating the co-movement nexus between air quality, temperature, and COVID-19 in California: implications for Public Health. *Front Public Health*. <https://doi.org/10.3389/fpubh.2021.815248>
- Ghazani M, Khosravi R, Barak S (2022) Nexus of COVID-19 and carbon prices in the EU emission trading system: evidence from multifractal and the wavelet coherence approaches. *Environ Sci Pollut R* 29(27):41293–41308. <https://doi.org/10.1007/s11356-021-18304-6>
- Gu H, Cao Y, Elahi E, Jha S (2019) Human health damages related to air pollution in China. *Environ Sci Pollut Res* 26(13):13115–13125. <https://doi.org/10.1007/s11356-019-04708-y>
- Habib Y, Xia E, Fareed Z, Hashmi S (2021) Time-frequency co-movement between COVID-19, crude oil prices, and atmospheric CO2 emissions: Fresh global insights from partial and multiple coherence approach. *Environ Dev Sustain* 23(6):9397–9417. <https://doi.org/10.1007/s10668-020-01031-2>
- Hakim Z, Archer-Nicholls S, Beig G, Folberth GA, Sudo K, Abraham NL, Ghude S, Henze DK, Archibald AT (2019) Evaluation of tropospheric ozone and ozone precursors in simulations from the HTAPII and CCM1 model intercomparisons- a focus on the Indian subcontinent. *Atmos Chem Phys* 19:6437–6458. <https://doi.org/10.5194/acp-19-6437-2019>
- He J, Gong S, Yu Y, Yu L, Wu L, Mao H, Song C, Zhao S, Liu H, Li X, Li R (2017) Air pollution characteristics and their relation to meteorological conditions during 2014–2015 in major Chinese cities. *Environ Pollut* 223:484–496. <https://doi.org/10.1016/j.envpol.2017.01.050>
- Huang Q, Chen G, Xu C, Jiang W, Su M (2021) Spatial Variation of the Effect of Multidimensional Urbanization on PM2.5 Concentration in the Beijing-Tianjin-Hebei (BTH) Urban Agglomeration. *Int J Environ Res Public Health*. <https://doi.org/10.3390/ijerph182212077>
- Hung N (2022) Biomass energy consumption and economic growth: insights from BRICS and developed countries. *Environ Sci Pollut Res* 29(20):30055–30072. <https://doi.org/10.1007/s11356-021-17721-x>
- Jia Z, Zhu C, Rajendran RS, Xia Q, Liu K, Zhang Y (2022) Impact of airborne total suspended particles (TSP) and fine particulate matter (PM2.5)-induced developmental toxicity in zebrafish (*Danio rerio*) embryos. *J Appl Toxicol*. <https://doi.org/10.1002/jat.4325>
- Jiang L, Bai L (2018) Spatio-temporal characteristics of urban air pollutions and their causal relationships: evidence from Beijing and its neighboring cities. *Sci Rep*. <https://doi.org/10.1038/s41598-017-18107-1>
- Katsavrias C, Papadimitriou C, Hillaris A, Balasis G (2022) Application of wavelet methods in the investigation of geospace disturbances: a review and an evaluation of the approach for quantifying wavelet power. *Atmosphere* 13(3):499. <https://doi.org/10.3390/atmos13030499>
- Khomsli K, Chelhaoui Y, Alilou S, Soury R, Najmi H, Souhaili Z (2022) Concurrent heat waves and extreme ozone (O-3) episodes: combined atmospheric patterns and impact on human health. *Int J Environ Res Public Health*. <https://doi.org/10.3390/ijerph19052770>
- Kumar R, Samuel C, Raju S, Gautam S (2022) Air pollution in five Indian megacities during the Christmas and New Year celebration amidst COVID-19 pandemic. *Stoch Environ Res Risk A*. <https://doi.org/10.1007/s00477-022-02214-1>
- Li X, Xia X, Wang L, Cai R, Zhao L, Feng Z, Ren Q, Zhao K (2015) The role of foehn in the formation of heavy air pollution events in Urumqi, China. *J Geophys Res-Atmos* 120(11):5371–5384. <https://doi.org/10.1002/2014JD022778>
- Li L, Lin Y, Xia T, Zhu Y (2020) Effects of electronic cigarettes on indoor air quality and health. *Annu Rev Publ Health* 41:363–380. <https://doi.org/10.1146/annurev-publhealth-040119-094043>
- Li H, Yang B, Wang L, Liao K, Sun N, Liu Y, Ma R, Yang X (2022a) A meta-analysis result: uneven influences of season, geo-spatial

- scale and latitude on relationship between meteorological factors and the COVID-19 transmission. *Environ Res.* <https://doi.org/10.1016/j.envres.2022.113297>
- Li K, Talifu D, Gao B, Zhang X, Wang W, Abulizi A, Wang X, Ding X, Liu H, Zhang Y (2022b) Temporal distribution and source apportionment of composition of ambient PM<sub>2.5</sub> in Urumqi, North-West China. *Atmosphere* 13(5):781. <https://doi.org/10.3390/atmos13050781>
- Liu Y, Wang T (2020) Worsening urban ozone pollution in China from 2013 to 2017-Part I: the complex and varying roles of meteorology. *Atmos Chem Phys* 20(11):6305–6321. <https://doi.org/10.5194/acp-20-6305-2020>
- Liu J, Kiesewetter G, Klimont Z, Cofala J, Heyes C, Schöpp W, Zhu T, Cao G, Sanabria AG, Sander R, Guo F, Zhang Q, Nguyen B, Bertok I, Rafaj P, Amann M (2019) Mitigation pathways of air pollution from residential emissions in the Beijing-Tianjin-Hebei region in China. *Environ Int* 125:236–244. <https://doi.org/10.1016/j.envint.2018.09.059>
- Lu J, Xie F, Tian H, Luo J (2021) Impacts of ozone changes in the tropopause layer on stratospheric water vapor. *Atmosphere.* <https://doi.org/10.3390/atmos12030291>
- Luo X, Sun K, Li L, Wu S, Yan D, Fu X, Luo H (2021) Impacts of urbanization process on PM<sub>2.5</sub> pollution in “2+ 26” cities. *J Clean Prod* 284:124761. <https://doi.org/10.1016/j.jclepro.2020.124761>
- Meng X, Wu Y, Pan Z, Wang H, Yin G, Zhao H (2019) Seasonal characteristics and particle-size distributions of particulate air pollutants in Urumqi. *Int J Environ Res Public Health.* <https://doi.org/10.3390/ijerph16030396>
- Naqvi HR, Mutreja G, Shakeel A, Karan S, Abbas K, Naqvi DF, Chaudhary AA, Siddiqui MA, Gautam AA, Gautam S, Naqvi AR (2022) Wildfire-induced pollution and its short-term impact on COVID-19 cases and mortality in California. *Gondwana Res.* <https://doi.org/10.1016/j.gr.2022.04.016>
- Pei T, Gao L, Yang C, Xu C, Tian Y, Song W (2021) The Impact of FDI on Urban PM<sub>2.5</sub> pollution in China: the mediating effect of industrial structure transformation. *Int J Environ Res Public Health.* <https://doi.org/10.3390/ijerph18179107>
- Ravina M, Esfandabadi ZS, Panepinto D, Zanetti M (2021) Traffic-induced atmospheric pollution during the COVID-19 lockdown: dispersion modeling based on traffic flow monitoring in Turin. *Italy J Clean Prod* 317:128425. <https://doi.org/10.1016/j.jclepro.2021.128425>
- Sheng Y, Simayi Z, Wang Y, Wang X, Li Y (2018) Spatiotemporal distribution pattern of ambient air pollution and its correlation with meteorological factors in Urumqi. *J Earth Environ* 9(4):323–333. <https://doi.org/10.13671/j.hjkxxb.2016.0105>
- Sofia D, Gioiella F, Lotrecchiano N, Giuliano A (2020) Mitigation strategies for reducing air pollution. *Environ Sci Pollut Res* 27(16):19226–19235. <https://doi.org/10.1007/s11356-020-08647-x>
- Wang J, Mo J, Li J, Ling Z, Huang T, Zhao Y, Zhang X, Mao X, Gao H, Shen Y, Ma J (2017) OMI-measured SO<sub>2</sub> in a large-scale national energy industrial base and its effect on the capital city of Xinjiang, Northwest China. *Atmos Environ* 167:159–169. <https://doi.org/10.1016/j.atmosenv.2017.08.002>
- Wang J, Wang D, Ge B, Lin W, Ji D, Pan X, Li J, Wang Z (2022) Increase in daytime ozone exposure due to nighttime accumulation in a typical city in eastern China during 2014–2020. *Atmos Pollut Res.* <https://doi.org/10.1016/j.apr.2022.101387>
- Wen L, Yang C, Liao X, Zhang Y, Chai X, Gao W, Guo S, Bi Y, Tsang S, Chen Z, Qi Z, Cai Z (2022) Investigation of PM<sub>2.5</sub> pollution during COVID-19 pandemic in Guangzhou, China. *J Environ Sci* 115:443–452. <https://doi.org/10.1016/j.jes.2021.07.009>
- Wu H, Gai Z, Guo Y, Li Y, Hao Y, Lu Z (2020) Does environmental pollution inhibit urbanization in China? A new perspective through residents’ medical and health costs. *Environ Res.* <https://doi.org/10.1016/j.envres.2020.109128>
- Xu L, Batterman S, Chen F, Li J, Zhong X, Feng Y, Rao Q, Chen F (2017) Spatiotemporal characteristics of PM<sub>2.5</sub> and PIV10 at urban and corresponding background sites in 23 cities in China. *Sci Total Environ* 599:2074–2084. <https://doi.org/10.1016/j.scitotenv.2017.05.048>
- Xu W, Wang Y, Sun S, Yao L, Li T, Fu X (2022) Spatiotemporal heterogeneity of PM<sub>2.5</sub> and its driving difference comparison associated with urbanization in China’s multiple urban agglomerations. *Environ Sci Pollut Res* 29(20):29689–29703. <https://doi.org/10.1007/s11356-021-17929-x>
- Yang Q, Yuan Q, Li T, Shen H, Zhang L (2017) The relationships between PM<sub>2.5</sub> and meteorological factors in China: seasonal and regional variations. *Int J Environ Res Public Health.* <https://doi.org/10.3390/ijerph14121510>
- Yin Z, Cui K, Chen S, Zhao Y, Chao H, Chang-Chien G (2019) Characterization of the Air Quality Index for Urumqi and Turfan Cities. *China Aerosol Air Qual Res* 19(2):282–306. <https://doi.org/10.4209/aaqr.2018.11.0410>
- Zeng X, Liu D, Wu W (2022) <p>PM<sub>2.5</sub> exposure and pediatric health in e-waste dismantling areas</p>. *Environ Toxicol Phar.* <https://doi.org/10.1007/s11356-021-17929-x>
- Zhang J, Wei Y, Fang Z (2019) Ozone pollution: a major health hazard worldwide. *Front Immunol* 10:2518. <https://doi.org/10.3389/fimmu.2019.02518>
- Zhang X, Gu X, Cheng C, Yang D (2020) Spatiotemporal heterogeneity of PM<sub>2.5</sub> and its relationship with urbanization in North China from 2000 to 2017. *Sci Total Environ.* <https://doi.org/10.1016/j.scitotenv.2020.140925>
- Zhang X, Ding X, Talifu D, Wang X, Abulizi A, Maihemuti M, Rekefu S (2021) Humidity and PM<sub>2.5</sub> composition determine atmospheric light extinction in the arid region of northwest China. *J Environ Sci* 100:279–286. <https://doi.org/10.1016/j.jes.2020.07.007>

**Publisher’s Note** Springer Nature remains neutral with regard to jurisdictional claims in published maps and institutional affiliations.

Springer Nature or its licensor (e.g. a society or other partner) holds exclusive rights to this article under a publishing agreement with the author(s) or other rightsholder(s); author self-archiving of the accepted manuscript version of this article is solely governed by the terms of such publishing agreement and applicable law.